Desalination and Water Treatment
www.deswater.com

doi: 10.1080/19443994.2015.1136695

57 (2016) 23814–23826
October

Taylor & Francis
Taylor & Francis Group

Effective removal of Hg^{2+} from aqueous solutions and seawater by *Malva sylvestris*

Bahman Ramavandi[a,b,*], Alireza Rahbar[c], Soleyman Sahebi[d,*]

[a]*Faculty of Health, Department of Environmental Health Engineering, Bushehr University of Medical Sciences, Bushehr 7518759577, Iran, Tel. +98 9363311903; Fax +98 77334550134; emails: ramavandi_b@yahoo.com, b.ramavandi@bpums.ac.ir*
[b]*Systems Environmental Health, Oil, Gas and Energy Research Center, Bushehr University of Medical Sciences, Bushehr, Iran*
[c]*Faculty of Health, Department of Nutrition, Bushehr University of Medical Sciences, Bushehr, Iran, email: rahbar_alireza@yahoo.com*
[d]*School of Civil and Environmental Engineering, University of Technology, Sydney (UTS), P.O. Box 129, Broadway, Sydney, NSW 2007, Australia, Tel. +61 295142647; email: soleysahebi@gmail.com*

Received 11 August 2015; Accepted 21 December 2015

ABSTRACT

This paper introduces a biomaterial prepared from *Malva sylvestris* for environmental remediation and medicine treatment purposes. The effects of pH (2–12), adsorbent dose (0.1–1.25 mg/L), Hg^{2+} concentration (5–15 mg/L), and contact time (3–60 min) were studied on the removal of Hg^{2+} from aqueous phase. The results were compared with powder of charcoal tablet, a medicine drug. At pH solution of 8, over 96% removal of 10 mg/L Hg^{2+} was obtained for a *M. sylvestris* powder (MSP) dose of 1.5 mg/L after a 40 min contact time; while for these conditions only 60% of Hg^{2+} was removed by charcoal tablet powder (CTP). The Langmuir model was the best fit for the experimental data, which attains a maximum adsorption capacity of 602 and 389 mg/g for MSP and CTP, respectively. Surface analyses (Fourier transform infrared, scanning electron microscopy, Brunauer, Emmet, and Teller, and X-ray photoelectron spectroscopy) of the MSP were also performed. The co-adsorption study indicated that the Hg^{2+} adsorption by MSP was 33% increased by addition of 2 mg/L ceftriaxone antibiotic. The MSP had acceptable performance after four times recycling. The MSP could be used to remove Hg^{2+} ions from seawater. Accordingly, the finding of this work suggests that the prepared adsorbent, MSP, is an efficient, no-cost, and promising biomaterial for the removal of Hg^{2+} ion from liquid phase and could be substituted for charcoal tablets in medicine.

Keywords: Ceftriaxone antibiotic; Co-adsorption; Hg^{2+} ion; *Malva sylvestris*; Seawater

1. Introduction

Adsorbents are widely applied for many purposes such as pollutant remediation [1–3], environmental sampling [4], analysis [5], food industries [6,7], and medicine [8]. In the field of medicine, adsorbents have been used from 50 years ago for treating illness such as heavy metal poisoning and bloating [9], and activated carbon or charcoal is the most widely used adsorbent. Charcoal is the first footsteps in the algorithm of heavy metal poisoning treatment. Commercially available activated carbon is still considered

---

*Corresponding authors.

expensive owing to the use of relatively expensive and non-renewable starting materials, such as coal. Further, the production of activated carbon is complex and expensive, making adsorption technology economically non-efficient. To make the adsorption method attractive and feasible, novel low-cost adsorbents with higher adsorption capacities are required. This has led to a growing research interest in the production of new adsorbents from renewable and no-cost precursors. Therefore, many biological materials, agricultural residues, waste materials, and self-growing plants can be investigated for the production of potential adsorbents. For instances, agricultural and waste materials have recently been viewed as potential low-cost adsorbents, and many reports have been published showing their ability to remedy various contaminants including heavy metals (for example, [10,11]). The grass of *Malva sylvestris* is proposed as a no-cost and profoundly accessible potential adsorbent.

To evaluate the adsorption potential of *M. sylvestris* for capturing adsorbates from aqueous solutions, Hg^{2+} ions were selected as a model pollutant; several biochars have been studied using Hg^{2+} as the model contaminant. Among the biochars tested over the past decade, some biochars like rice husk ash [12] and sugarcane bagasse [13] have presented considerable adsorption capacity. However, the application of these biochars is restricted practically because the adsorbent is not available in great enough amounts. In the other words, despite having a significant capacity for pollutant adsorption, most of these materials are not produced in a central location in one country; therefore, they are not available in sufficient bulk to be commercialized for full scale application. Indeed, a candidate biochars that can act as an option to activated carbon/charcoal must both have a high adsorption capacity and be abundantly available in bulk at no or low cost. In this context, *M. sylvestris* was proposed to be assessed for its potential to adsorb Hg^{2+}. *M. sylvestris* has been considered because it is a self-seeding, fast growing, and common plant that grows mainly throughout Iran, especially in the surrounding area of Bushehr city and is easily prepared and used. It is a small, annual plant, with hollow stems, and a height of up to 0.5 m, from the *Malvaceae* family. *M. sylvestris* may be one of the world's oldest plant foods known to humans, especially in Mediterranean and Middle Eastern countries. This plant is used in traditional medicine for curing toothache, belly pain, cystitis, cough, cold, and bronchitis [9]. In animal models, *M. sylvestris* presented an antinociceptive effect, in skin inflammatory condition, anti-inflammatory action in mucous membranes, and in carrageenan-induced paw edema when topically applied [14,15].

To the best of the authors' knowledge, no publicly funded research has yet studied the use of *M. sylvestris* in applications such as water and wastewater treatment and heavy metal detoxifying. Therefore, it is very interesting to test the potential of *M. sylvestris* to remove Hg^{2+} ion from aqueous solutions. The aim of the present study was to explore the potential of *M. sylvestris* to remove a model pollutant, Hg^{2+} ions, from aqueous solution and seawater under different operational parameters. The effects of the main parameters, that is, solution pH, adsorbent dose, adsorbate concentration, contact time, and solution temperature were explored for Hg^{2+} removal. The co-adsorption of Hg^{2+} and ceftriaxone antibiotic and the surface analysis of MSP were also studied.

2. Experimental

2.1. Materials

The *M. sylvestris* powder (MSP) was prepared from leaves and stems of *M. sylvestris* as follows: First, *M. sylvestris*, was obtained from the north of Bushehr Province, Iran. Then the samples of *M. sylvestris* were air-dried for three consecutive days and powdered using a grinder to obtain the particle size of mesh 200. Finally, the prepared powder was put an oven at a temperature of 500°C under air and kept at this temperature for 2 h. Thereafter, the resulting MSP was put in a capped glass vessel for use as an adsorbent as required. The charcoal tablet was supplied from a local pharmacy. The tablet was grinded and powdered and sieved to mesh size of 200 to obtain charcoal tablet powder (CTP). The main properties of CTP are presented in Table 1. The ceftriaxone (CF) antibiotic with analytical grade was provided from Sigma Aldrich Co., and used as received. The characteristics of CF are listed in Table 2.

2.2. Experimental procedure

Hg^{2+} removal tests with the prepared MSP and CTP were conducted as a batch test in 100-mL flask

Table 1
Main characteristics of CTP

Characteristic	Unit	Value
BET	m^2/g	972
Total pore volume	cm^3/g	0.0011
Average pore diameter	nm	0.68
BET constant *C*	–	328
pH_{zpc}	–	8.1
Total ash	%	1.64
Particle size	Mesh	200

Table 2
Main properties of ceftriaxone antibiotic used in this study

Parameter	Unit	Character/value
Molecular structure	–	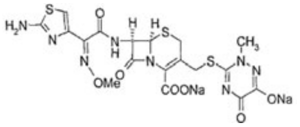
CAS number	–	74,578-69-1
Molecular formula	–	$C_{18}H_{16}N_8Na_2O_7S_3$
Molar mass	g/mol	661.59
Solubility in water	g/L at 25 ℃	400
Dissociation constant (pK_a)	–	~3(COOH), 3.2(NH_3^+), and 4.1(enolic OH)

while agitating on a shaker–incubator instrument (Parsazma Co., Iran). Each test consisted of preparing 50 mL of Hg^{2+} solution with a given initial concentration, and the initial pH of the solution was adjusted by adding 0.1 N HCl and NaOH solutions. Thirty milliliter aliquots of the samples were then filtered through 0.45-μm filters at determined time intervals. The percentage of removal and the amount of adsorption at equilibrium, q_e (mg/g), by MSP and CTP were obtained by the following equations:

$$\text{Adsorption}\,(\%) = \frac{C_0 - C_f}{C_0} \times 100 \tag{1}$$

$$q_e = \frac{C_0 - C_e}{W} \times V \tag{2}$$

where C_0, C_f, and C_e (mg/L) are adsorbate concentrations at initial, final, and equilibrium, respectively. V (L) is the solution volume, and W (g) is the dry mass of adsorbents.

The pH, adsorbent dosage, initial adsorbate concentration, and contact time were the variables in this work. The experimental runs and the corresponding conditions are presented in Table 3. All tests were done in triplicate to ensure the reproducibility of data, and the average values are stated. Control tests containing no MSP or CTP were also performed.

To assess the isotherms of Hg^{2+} adsorption onto CTP or MSP, a series of tests were conducted. The quantity of 100 mL of a solution containing 5–35 mg/L of Hg^{2+} with a pH of 8 was poured into seven flasks. Thereafter, 1 g of MSP or CTP was added to each flask. The flasks were subsequently stirred at an adjusted temperature (24℃) for 1,440 min at 120 rpm to achieve equilibrium. Finally, the suspensions were filtered using the Whatman filter, and the filtrates were analyzed for residual Hg^{2+}.

To do reusability tests, the MSP and CTP were regenerated for four consecutive cycles by using 1 mol/L HCl solution. The regenerated adsorbent was then subjected to Hg^{2+} adsorption under the experimental conditions presented in Table 3.

The impact of MSP and CTP on mercury ions adsorption from a complex matrix (seawater) was also studied. To do this, a bulk quantity of seawater was supplied from the Persian Gulf and spiked with 10 mg/L Hg^{2+}. No other properties of the seawater were adjusted and spiked to given value. The seawater, consisting of both organic and inorganic substances, was alkaline (pH 8.1) in nature. In this section, the tests were carried out under the conditions that were determined in Table 3.

2.3. *Adsorbent characterization and analytical methods*

The characterizations of the MSP were determined by assessing the pH of zero point charge (pH_{zpc}), specific surface area, pore volume and size, surface functional groups, and surface morphology. The specific surface area based on the Brunauer–Emmet–Teller (BET) method. The pore volume was calculated by Micromeretics/Gemini-2372. The mean pore diameter was determined using BET, and the total pore volume was measured using the method stated by Altenor et al. [16]. The structural surface of the prepared adsorbent was determined by scanning electron microscopy (SEM) (Philips XL-30). The functional groups present on the surface of the MSP were identified by Fourier transform infrared (FTIR) spectroscopy (Shimadzu 4300). The X-ray photoelectron spectroscopy (XPS) analysis was performed with an AXIS-Ultra instrument from Kratos Analytical using monochromatic Al Kα radiation (15 mA, 225 W, 15 kV) and low energy electron flooding for charge adjustment. To adjust the surface charge impacts, binding energy was

Table 3
Experimental runs and conditions

Run	Experiment	Experimental conditions: pH	Hg^{2+} concentration (mg/L)	Adsorbent dose (mg/L)	Contact time (min)	Temperature (℃)
1	Effects of solution pH	2–12	5	1	40	24
2	Effects of adsorbent dose	8	10	0.1–1.25	40	24
3	Effects of Hg^{2+} concentration and contact time	8	5–15	1	3–60	24
4	Co-adsorption of Hg^{2+} and ceftriaxone antibiotic	8	15	0.5	40	24
5	Adsorption isotherm	8	5–35	1	1,440	24
6	Effects of solution temperature	8	10	1	40	5–35
7	Reusability study	8	10	1	40	24
8	Removal of Hg^{2+} from the complex matrix (seawater)	As original (8.1)	10	1	40	24

controlled using C1s hydrocarbon peak at the binding energy of 284.80 eV. The information was first converted into VAMAS file format and then imported into CASAXPS software for manipulation and curve fitting.

The concentration of Hg^{2+} ion in solutions was measured using atomic absorption spectroscopy (Atomic Absorption/Flame Emission Spectrophotometer Shimadzu AA-670). The solution pH was determined using a pH meter (Sense Ion 378, Hack). The solution temperature was measured by a mercury thermometer. The level of ceftriaxone sodium was determined using liquid chromatography (Agilient 1100, USA). The mobile phase was of a mixture of acetonitrile (73:27, v:v) and 0.02 mol/L N-octyl amine and the wavelength of 254 nm was applied to detect ceftriaxone sodium with a flow rate of 1 mL/min.

The paired *t*-test statistical analysis at a 95% confidence level ($p < 0.05$) was used to compare the Hg^{2+} removal efficiency of MSP and CTP. The statistical analysis was performed using SPSS software version 22.

3. Results and discussion

3.1. Characteristics of charcoal

Surface analysis indicated that MSP had a BET multipoint surface area of 2.34 m^2/g and a total pore volume at 0.9925 P/P_0 of 0.0002 cm^3/g. BET constant C of MSP was achieved 846, indicating the affinity of MSP to uptake Hg^{2+} ions from solutions. According to the calculations, the average size of pores was 0.78 nm, confirming that MSP was a microporous adsorbent. Because the specific surface area of MSP is low, the functional groups are likely have a more pronounced role than BET [17] in adsorbing mercury ions from solutions. The surface structures of the original and Hg-loaded MSP imaged at the same magnification are presented in Fig. 1. As shown in Fig. 1(a), the original MSP was a porous material with a smooth surface. Fig. 1(b) depicts MSP after adsorption, indicating that mercury ions are adsorbed evenly on the surface of MSP. The EDX analysis of adsorbent before and after Hg^{2+} adsorption (data not shown) confirmed this observation. The presence of mercury on MSP (~84 wt.%) showed that the mercury ions removed from solution had been adsorbed onto MSP. The pHzpc of the prepared biochar, MSP, was determined from the titration curve to be approximately 7.3, signifying a positive surface charge for a solution pH < 7.3 and a negative surface charge for a solution pH > 7.3.

The chemical structure of adsorbents is very important in understanding the adsorption process. The FTIR technique is a useful tool to identify the characteristic functional groups. In Fig. 2, the functional groups of fresh MSP and Hg^{2+}-adsorbed MSP and the corresponding infrared adsorption bands are presented. As shown in Fig. 2 and on the basis of the existing literature [17], it is known that the spectra display a number of adsorption peaks, indicating the active functional groups on the MSP surface. These peak shifts after adsorption indicate that the bonded –OH, $–NH_2$, –C–H, and –COOH functional groups play a key role in Hg^{2+} adsorption onto the MSP. The main changes in the band between 2,800 and 3,500 cm^{-1} after the adsorption of Hg^{2+} indicate the chemisorption processes predominantly involved in the adsorption of Hg^{2+} by the MSP. The disappearance

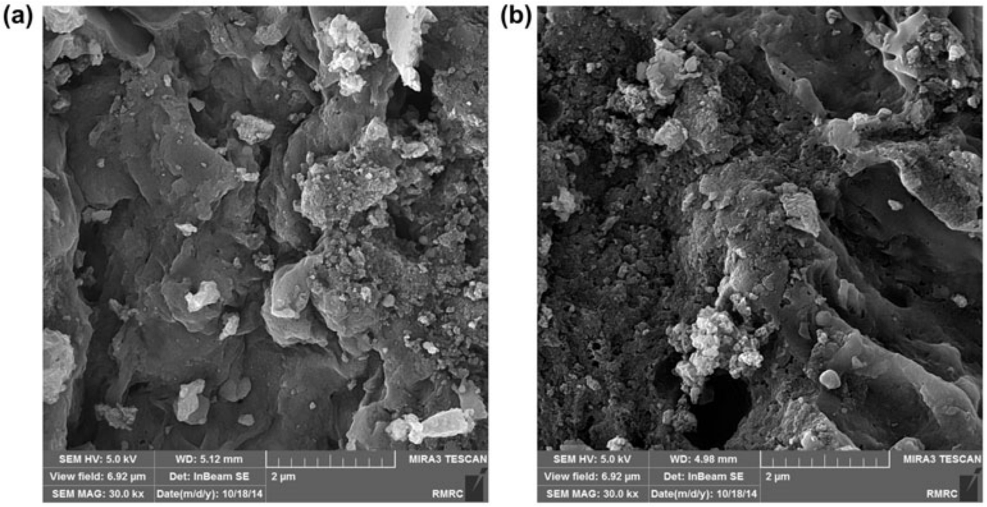

Fig. 1. SEM micrograph of (a) fresh and (b) Hg^{2+}-loaded MSP.

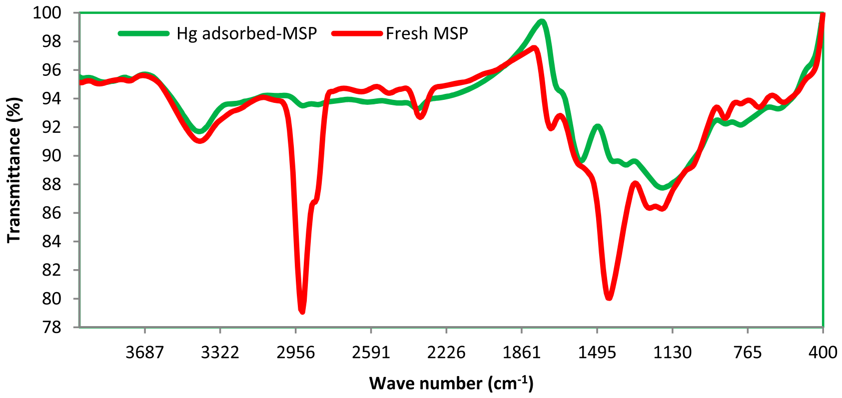

Fig. 2. FTIR spectra of MSP at wave numbers from 400 to 4,000 cm^{-1}.

of the peaks 2,931.27 and 1,450.2 cm^{-1} after mercury ions adsorption might demonstrate that the corresponding functional groups (that is, –C–H and–COOH) are completely involved in the adsorption process. This result also implies that a complex C, N, and O atoms of the functional groups of the MSP surface is involved in adsorbing Hg^{2+} [18].

3.2. Effects of solution pH

Since the pH of the aqueous solution plays an important role in the adsorption process, in Run 1 experiments, the effect of solution pH on the removal of Hg^{2+} by MSP was examined under the conditions presented in Table 3. The adsorption pH was tested in a range of 2–12 and to avoid the formation of mercury hydroxide precipitation at alkaline condition, the experiments were performed using Hg^{2+} concentration of 5 mg/L [19]. The results of pH effect on Hg^{2+} removal are presented in Fig. 3. This figure clearly indicates that the adsorption of Hg^{2+} was highly affected by the solution pH. Similar observations were stated for Hg^{2+} adsorption onto different adsorbents by other authors [2,20–22]. As seen from Fig. 3, both adsorbents (MSP and CTP) had a same trend for adsorption of Hg^{2+} ions, however, the efficiency of MSP was more notable than CTP. Under acidic conditions, the lowest amounts of Hg^{2+} were adsorbed. Fig. 3 also shows that Hg^{2+} adsorption onto the MSP increased from 34 to 100% when the pH solution increased from 6 to 10. It can be said that at acidic conditions, the amount of negatively charged surface sites decreases and the amount of positively charged sites increases due to the protonation effect. Under these conditions, the adsorption of positively charged Hg^{2+} ions is restricted due to electrostatic repulsion.

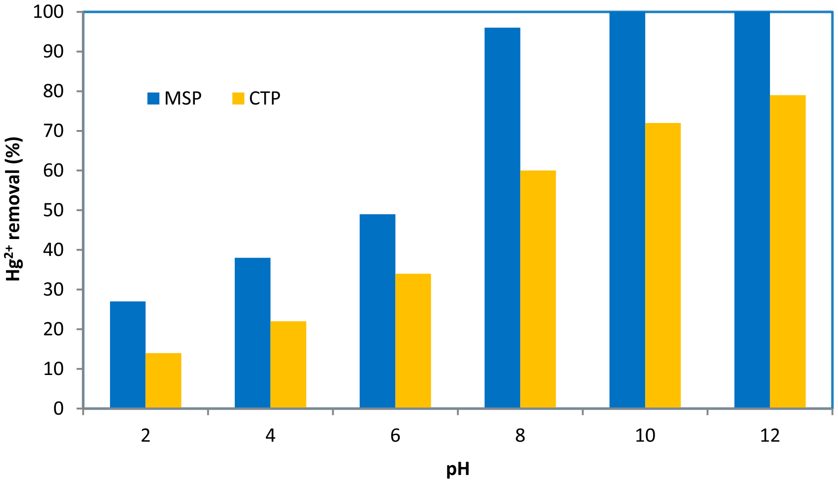

Fig. 3. Effect of pH on Hg^{2+} adsorption by MSP and CTP.

Further, the presence of excess H^+ ions, causes lowering of Hg^{2+} adsorption due to competing between H^+ and Hg^{2+} ions for accommodation the adsorption sites. Therefore, at high pH values, due to less competition for occupying of adsorption sites, the degree of protonation of the surface gradually reduces and the adsorption efficiency increases [3,23].

3.3. Effects of adsorbent dose

The effect of adsorbent dose (0.1–1.25 mg/L) on mercury adsorption was studied in under the conditions specified in Table 3. The results are presented in Fig. 4. As can be seen from Fig. 4, at the adsorbent dose of 1.25 mg/L the mercury ions were completely removed by MSP while only 67% Hg^{2+} was removed by CTP at this dose. This is one of the advantages of MSP in comparison with CTP. The increasing of Hg^{2+} adsorption by increasing of both adsorbents dose could be explained by the greater availability of active binding sites and to the presence of a greater surface area for adsorption.

From Fig. 4, increasing the CTP dosage from 0.1 to 0.75 mg/L increases the percentage of Hg^{2+} removal from 22 to 56% after 40 min contact time, while with further increases in the CTP doses the percentage of Hg^{2+} removal exhibited no significant increase. One plausible reason could be due to the overlap of active sites at higher CTP doses, resulting in decreased effective surface area required for Hg^{2+} adsorption [24,25].

3.4. Effects of Hg^{2+} concentration and contact time

The effect of varying initial Hg^{2+} concentration from 5 to 15 mg/L on adsorption was studied under the conditions provided in Table 3. Fig. 5 presents the average results of duplicated examinations. According to Fig. 5, the adsorption efficiency of Hg^{2+} was notably greater for adsorption onto MSP that onto CTP, reconfirming the better performance of MSP to remove Hg^{2+} compared with CTP. Maximum removal of Hg^{2+} at the initial concentration of 5 mg/L by MSP and CTP was 100 and 69%; maximum removal efficiencies decreased to 93% (by MSP) and 58% (by CTP) when the initial Hg^{2+} concentration was increased to 15 mg/L. Generally, the rate of adsorption process was higher within the first 10 min of contact time for both adsorbents. Based on data illustrated in Fig. 5(a), by increasing the contact time to 60 min, the mercury ion removal were obtained 93, 98, and 100% for initial Hg^{2+} concentrations of 5, 10, and 15 mg/l, respectively. Considering that the concentration of adsorbents (MSP or CTP) was constant during the tests (1 mg/L), the decrease in removal efficiency with

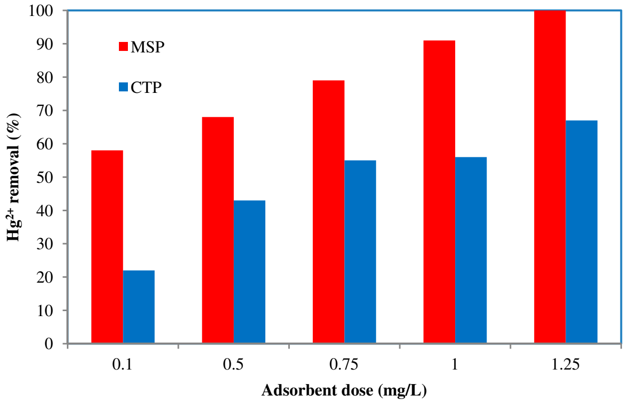

Fig. 4. Effect of adsorbent dose on Hg^{2+} removal.

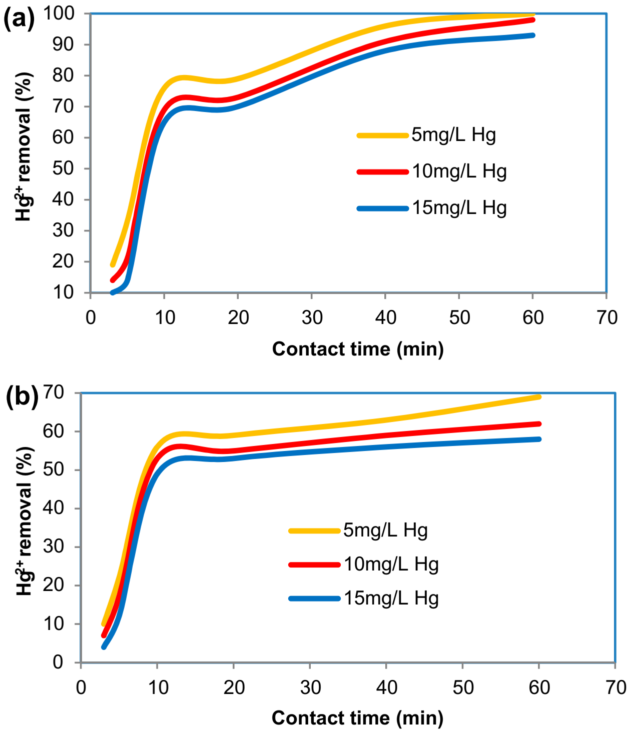

Fig. 5. Effect of Hg^{2+} concentration on Hg^{2+} removal by (a) MSP and (b) CTP as a function of contact time.

increased Hg^{2+} concentration could be accounted to limited availability of adsorption sites for increased amounts of Hg^{2+} ions [26,27]. These results are in accordance with those of other research. For example, Wang et al. [28] and Moussavi et al. [29] stated a similar trend of changing adsorption efficiency as a function of initial pollutant concentration, although experiments were carried out with a different adsorbent and adsrobate. These findings imply higher affinity and thus favorability of MSP for adsorbing Hg^{2+} from aqueous solutions.

3.5. *Co-adsorption of Hg^{2+} and ceftriaxone antibiotic onto MSP*

The co-adsorption of ceftriaxone (CF) and Hg^{2+} onto MSP in different concentrations of CF solutions was studied according to conditions indicated in Table 3. As shown in Fig. 6, Hg^{2+} adsorption by MSP was significantly improved in the presence of CF, while Hg^{2+} adsorption by CTP was suppressed by the addition of CF. From Fig. 6(a), at the contact time of 60 min the removal percentage of Hg^{2+} was increased to 17 and 36% when 0.5 and 2 mg/L CF was present in the solution, respectively. This is further evidence for showing the superiority of the MSP to the CTP. The adsorption of CF provided additional adsorption sites for Hg^{2+} by complexation, forming tertiary surface complexes MSP–Hg^{2+}–CF.

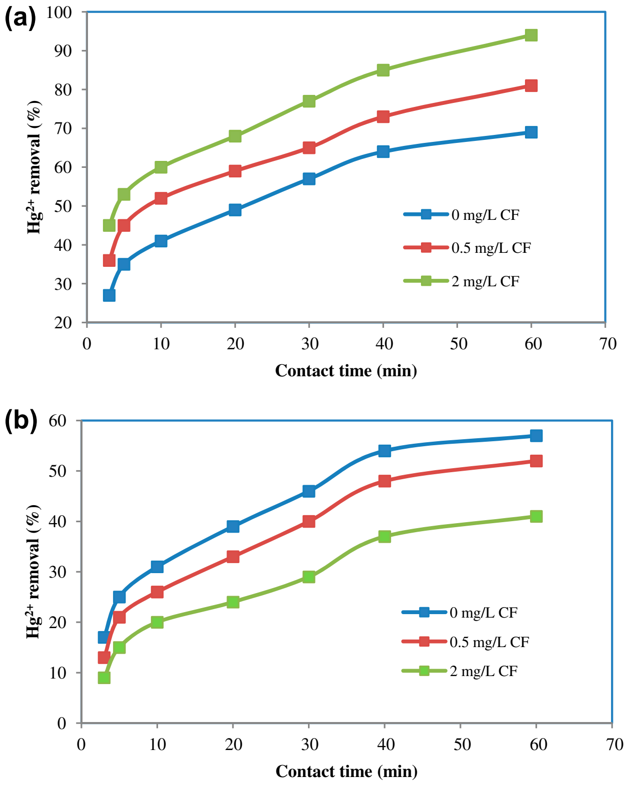

Fig. 6. Co-adsorption of Hg^{2+} and CF onto (a) MSP (b) CTP.

The co-adsorption of heavy metal ions and organics onto adsorbents, such possible reasons for the enhancement effect, as the higher affinity of the complex and the creation of new sites of the efficient bridge, were all described in the literatures [30,31]. To further reveal the roles of CF in Hg^{2+} adsorption onto MSP in the binary system, the XPS analysis of the MSP after the adsorption of Hg^{2+} and Hg^{2+}–CF were conducted (see Fig. 7). Herein, the complexation between CF and Hg^{2+} has been demonstrated by XPS spectroscopic analysis, suggesting that [Hg-CF] complex could be adsorbed with a higher affinity to the solid phase (Route I, Fig. 8). On the other hand, surface complex interaction of Hg^{2+} and CF on solid phase could also occur, in which CF offered new active sites to effectively bridge for Hg^{2+} adsorption (Route II, Fig. 8). Each of the two routes possibly strengthened the adsorption of Hg^{2+} on MSP in binary systems. A wide scan of MSP–CF–Hg samples was presented in Fig. 7(a). Except the major elements C1s, O1s of the MSP, clear S2p, N1s, Hg4p peaks successively occurred at around 164.0, 397.9, and 932.6 eV, which provided sufficient evidence of the

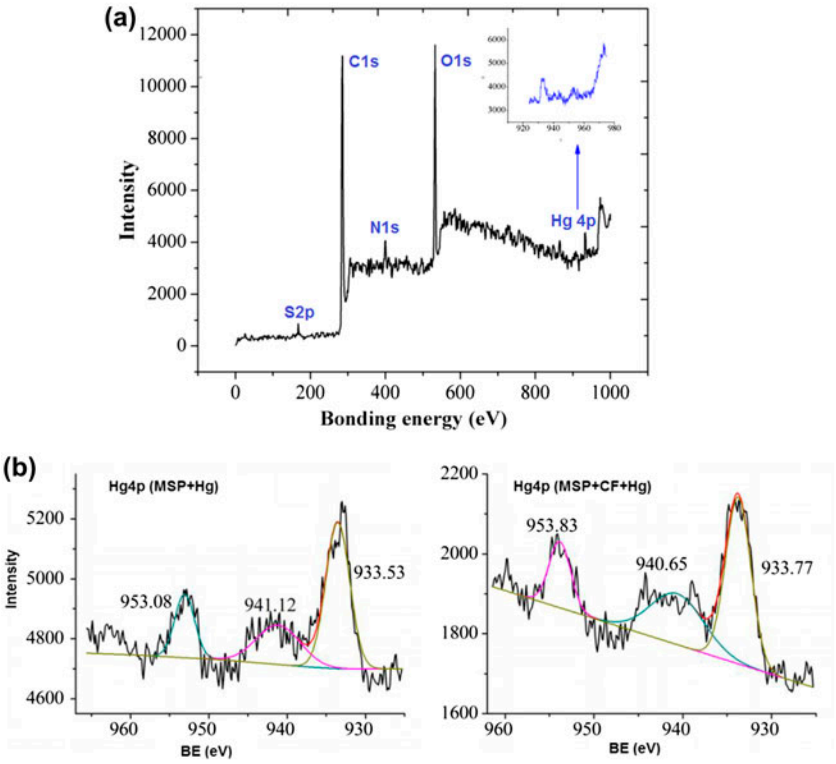

Fig. 7. (a) XPS wide scan of MSP + CF + Hg (the peak of Hg4p was amplified) and (b) XPS spectra of Hg4p in the samples of MSP + Hg and MSP + CF + Hg.

co-adsorption of CF and Hg^{2+} onto the adsorbent [30]. In the Hg4p spectra (Fig. 7b), a satellite band (940.57–941.60 eV) was observed nearby the Hg4p peak (933.53–933.76 eV), which was representative of the oxidation state of Hg^{2+} [32]. On MSP, the presence of CF induced the shift of the Hg 4p peak from 933.53 eV to 933.77 eV due to the formation of Hg^{2+}–CF complex. The XPS analysis showed that Hg^{2+} and CF formed complexes at the interface of the MSP, thereby enhancing their removal from the aqueous solution.

According to the above explanations, the complex of [MSP-CT] (Route I) and surface complex interaction between mercury ions in aqueous phase and MSP surface (Route II) were both possible mechanisms for the synergistic effect. Herein, the possible mechanisms for enhanced adsorption of Hg^{2+} and CF onto MSP are depicted in Fig. 8. Further, Route II was confirmed to be superior, particularly in high concentration of CF. Two types of sites newly supplied by CF on the surface of MSP were identified to contribute jointly to the complex-interaction of mercury ions and MSP–CF; one of them was –COOH group (Site I) and the other was $–NH_2$ group (Site II). The mercury ions were removed by the former through ion-exchange mechanism, and the latter though coordination one.

3.6. MSP capacity for Hg^{2+} removal

An isotherm represents the relationship between amounts of Hg^{2+} adsorbed onto adsorbent at given experimental conditions and the equilibrium concentration of the adsorbate in the liquid phase. Therefore, an isotherm would be informative for determining the maximum capacity of adsorbent for the adsorbate, designing an optimized adsorption process, and determining the main mechanism involved in the adsorption process. In this regard, the conformity of experimental data with three of the most used isotherm models (Langmuir, Freundlich, and Dubinin–Radushkevich) was evaluated. The linear forms of the equations are provided below:

$$\frac{C_e}{q_e} = \frac{1}{b\,q_{\max}} + \frac{C_e}{q_{\max}} \tag{3}$$

where $q_{\max}$ (mg/g) represents the maximum adsorption capacity. The parameter b represents a coefficient related to the energy of adsorption and increases with an increase in the strength of adsorption.

$$\ln q_e = \ln K_F + \frac{1}{n}\ln C_e \tag{4}$$

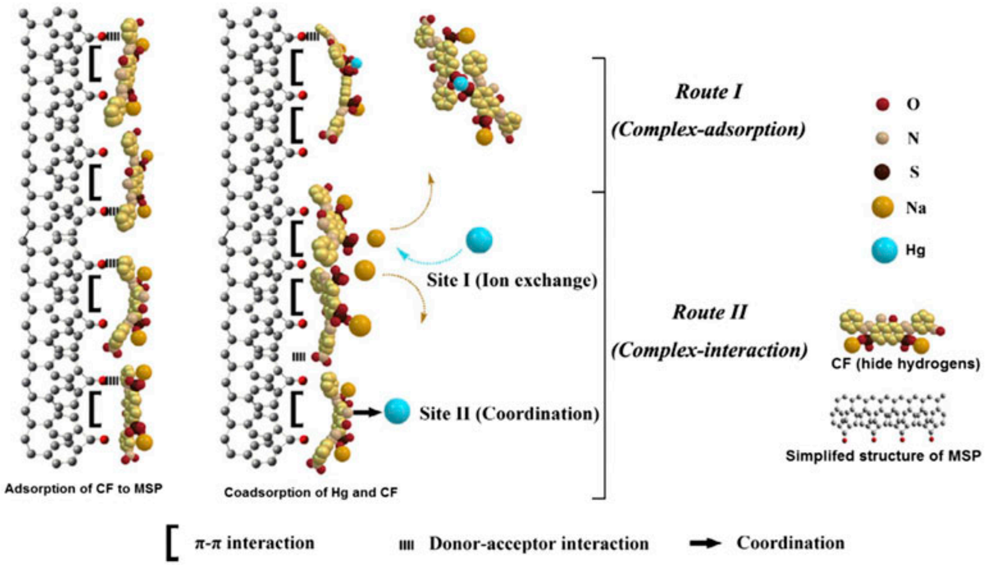

Fig. 8. Possible mechanisms for co-adsorption of Hg^{2+} and CF onto MSP (from reference [30] with little changes).

where K_F and n are the constants of the Freundlich model. K_F is the capacity of the adsorbent for the adsorbate, and $1/n$ is the reciprocal of the reaction order, which is a function of the strength of adsorption.

$$\ln q_e = \ln q_m - K_{DR}\, \varepsilon^2 \quad (5)$$

where q_m represents the maximum adsorption capacity (mg/g); K_{DR} represents a constant (mol^2/kJ^2); and ε represents the Polanyi potential (J/mol).

The information obtained from isotherm modeling was summarized in Table 4. As can be seen, from the correlation coefficient (R^2) values the Langmuir model exhibited the best fit for the adsorption equilibrium experimental data for both adsorbents, which very well implies the monolayer adsorption pattern on an energetically uniform surface. The suitability of the adsorption process could be evaluated by calculating the separation factor constant ($R_L = (1/(1 + C_0 b))$: $R_L > 1.0$, unsuitable; $R_L = 1$, linear; $0 < R_L < 1$, suitable; $R_L = 0$, irreversible [25]. The values of R_L lie between 0.3731 and 0.8064, indicating the suitability of the MSP as adsorbents for Hg^{2+} from aqueous solution. Further, the value of the constant n in the Freundlich model, included in Table 4, was much greater than unity, which also verifies that MSP is an appropriate adsorbent for the removal of Hg^{2+} from aqueous solutions.

The q_{max} values for MSP and CTP attained were 602 and 389 mg/g, respectively. The greater Hg^{2+} adsorption capacity of MSP than CTP (under similar conditions) can further be described by considering the BET constant C. The BET constant C is related to the adsorption energy in the first adsorbed layer. Accordingly, the value of C represents the magnitude of interactions between Hg^{2+} ions and adsorbents; the greater the BET constant C value the greater the interactions between Hg^{2+} ions and adsorbent, and thus the higher the adsorption rate and capacity. The values of BET constant C for CTP and MSP are 327 and 846, respectively, indicating that Hg^{2+} had a significantly greater interaction with the surface of MSP that of CTP resulting in greater adsorption of Hg^{2+} ions onto MSP than onto CTP. The greater interaction between Hg^{2+} and the MSP than the CTP may be

Table 4
Isotherm parameters for the adsorption of Hg^{2+} by MSP and CTP

Isotherm	Parameters	MSP	CTP
Langmuir	q_{max} (mg/g)	602	389
	b (L/mg)	0.048	0.096
	R^2	0.998	0.993
	R_L	0.3731–0.8064	0.2293–0.6757
Freundlich	K_F	112.3	81.6
	n	4.2	2.6
	R^2	0.841	0.833
D–R	K_{DR}	0.0026	0.0108
	$E = (1/2K_{DR})^{0.5}$	13.8	6.8
	R^2	0.923	0.917

Table 5
Comparison of the maximum adsorption capacities of Hg^{2+} ions on different adsorbents

Adsorbents	q_{max} (mg/g)	Refs.
MSP	602	Current work
CTP	389	Current work
Thiol functional organoceramic	726	[1]
Activated carbon from waste	25.88	[32]
4-aminoantipyrine immobilized bentonite	52	[34]
Amine group-containing chelating fiber	857	[35]
Polystyrene modified with 2-amino-pyridine	31	[36]
Polyaniline/reduced graphene oxide	1,000	[37]
Marin macroalga	178	[38]
Chitosan foams	350	[39]
Chitosan	750	[40]

Table 6
Parameters of the Persian Gulf water after and before treatment by MSP and CTP

Parameters (mg/L)	Before treatment	After treatment by	
		MSP	CTP
pH	8.1	7.4	7.8
DOC	3.6	3.3	3.2
SO_4^{2-}	2,492	2,432	2,389
Cl^-	18,733	18,693	18,690
K^+	532	502	489
Mg^{2+}	1,381	1,308	1,291
Cu^{2+}	97	62	81
Ca^{2+}	445	438	437
[a]Hg^{2+}	10	3.88	8.17

[a]The background level for mercury ion of the Persian Gulf water was zero and the water was spiked with 10 mg/L Hg^{2+}.

related to the higher density of charge and surface functional groups in MSP compared to that in CTP (Fig. 2). It concludes that there are a greater number of available sites on the surface of MSP than on the CTP for interaction with the Hg^{2+} ions.

From Table 4, the q_{max} value of MSP was notably greater (54%) than those obtained for CTP, indicating MSP is a promising method for decontaminating mercury ions from aqueous solution. Further, the q_{max} value of MSP was higher than some q_{max} values of previously stated adsorbents (see Table 5). However, the adsorbents with higher amounts of q_{max} will not be potential alternative for possible applications in medicinal uses as these materials are synthetic and non-edible. Therefore, the advantages of MSP are high adsorption capacity, availability and abundance of the propellant material, and simplicity of preparation. These items make MSP as an economical and efficient adsorbent for separating Hg^{2+} from effluents.

Based on the results of the Dubinin–Radushkevich (D–R) model (Table 4), the amount of free energy in Hg^{2+} adsorption by MSP and CTP were 13.8 and 6.8 kJ/mol, respectively. A value of E between 8 and 16 kJ/mol and less than 8 kJ/mol indicates that chemisorption and physisorption are the dominant processes under the experimental conditions [33], respectively. Thus, the adsorption of Hg^{2+} by MSP

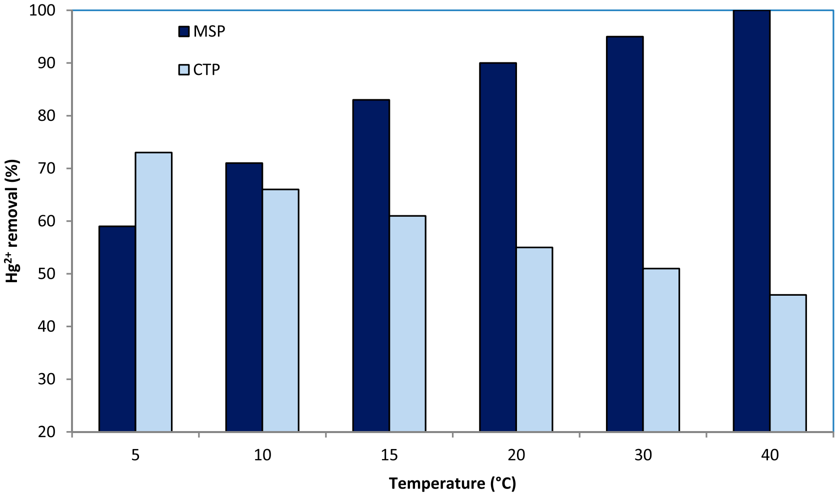

Fig. 9. Effect of solution temperature on Hg^{2+} removal by MSP and CTP.

Table 7
Reusability of MSP and CTP for Hg^{2+} removal from aqueous solution and seawater

	MSP		CTP	
Cycle of use	Aqueous solution	Seawater	Aqueous solution	Seawater
Fresh	93.4	61.2	57.8	18.3
1	90.2	54.8	53.4	12.1
2	85.6	48.4	46.5	3.7
3	79.9	38.5	40.1	0
4	70.1	27.8	31.8	0

occurs by a mechanism of chemisorption and the physisorption was the main mechanism for the target pollutant removal by CTP.

3.7. Effect of solution temperature

The adsorption of Hg^{2+} onto MSP and CTP was investigated at temperatures of 5, 10, 15, 20, 30, and 40°C at conditions given in Table 3. As presented in Fig. 9, different trends were found for the adsorption process for both adsorbents reaffirming that the adsorption process of mercury ions by both adsorbents was different. The increase in the solution temperature from 5 to 40°C leads to an increase in the mercury ions removal from 59 to 100%, respectively, by MSP. This may show that the adsorption of Hg^{2+} ions onto active sites of the MSP surface are endothermic and could be enhanced by availability of more active sites of the adsorbent, the enlargement and activation of the adsorbent surface at higher temperatures. Another plausible reason for the higher Hg^{2+} adsorption at the higher solution temperature is that the easy mobility of mercury ions from the solution to the MSP surface and thereby the enhanced accessibility to the adsorbent active sites. These results are supported by other researchers [41–43].

3.8. Removal of Hg^{2+} from the complex matrix (seawater)

To study the effects of seawater as a natural and complex matrix on the adsorption of mercury ions by MSP and CTP a test was performed under conditions given in Table 3. The seawater obtained from the Persian Gulf coast at Bushehr was filtered using 0.45 μm filter membrane and then stored in polyethylene bottles [44].The results are presented in Table 6. As can be seen, the removal percentage of Hg^{2+} from the seawater reached 61.2 and 18.3% for MSP and CTP, respectively, after 40 min. Further, from Table 6 not only Hg^{2+} ions were removed by MSP but other characteristics of sea water were also reduced during treatment. Other notes could be derived from Table 6 are that the efficiency of MSP was more than CTP for Hg^{2+} removal from seawater. The affinity of mercury ions for MSP was more than CTP as mercury ions removal by MSP was greater than the CTP. Based on the results, the MSP is a reliable and potential technique to capture Hg^{2+} ions from the natural sample.

3.9. Reusability of MSP and CTP

An important property of an adsorbent, from environmental and economical point of view, is its reusability potential. To evaluate the reusability of MSP and CTP in the adsorption of Hg^{2+} from both aqueous solution and seawater, an experimental phase was done according to conditions specified in Table 3. The mercury ions removal efficiencies that were monitored for four times recycling of MSP and CTP are presented in Table 7. As can be seen from Table 7, the MSP preserved its capability after four times recycling and the efficiency was still acceptable for Hg^{2+} removal from aqueous solution. It can be concluded that the MSP is more effective than CTP and can be used in multiple cycles for mercury removal from both aqueous solution and seawater.

4. Conclusions

In this work, a novel biochar was prepared from *M. sylvestris* and characterized using various instrumental techniques. The operating parameters consisted of pH, adsorbent dose, contact time, and Hg^{2+} concentration were found to be effective on the adsorption efficiency of Hg^{2+}. Co-adsorption studies showed that the presence of ceftriaxone antibiotic offers the advantages of synergy toward targeted Hg^{2+} ions by MSP. Also, the Langmuir isotherm model was fitted well with the experimental data, implying the monolayer adsorption of Hg^{2+} ions. The maximum capacity of MSP was determined to be 602 mg/g, which was much higher than that of the CTP, 389 mg/g, for Hg^{2+}

ion adsorption. The predominant mechanism for mercury ion removal by MSP and CTP was chemisorption and physisorption, respectively. The proposed adsorbent in this study was also applied to the adsorption of Hg^{2+} ion from seawater. Therefore, it is concluded that *M. sylvestris* is a viable and very promising alternative adsorbent for Hg^{2+} removal from aqueous solutions. The removal efficiency (by MSP) increased as temperature elevated. The results suggest that the MSP is a potential adsorbent to use in medicine for treatment of poisoning with heavy metals; however, the application in animal models is a necessary step before the eventual application of MSP in situations involving humans.

Acknowledgment

The authors would like to thanks the financially and technically support provided by the Bushehr University of Medical Sciences, Iran (Project no: BUMS-94-H-11) to conduct this work.

References

[1] K.H. Nam, S. Gomez-Salazar, L.L. Tavlarides, Mercury (II) adsorption from wastewaters using a thiol functional adsorbent, Ind. Eng. Chem. Res. 42 (2003) 1955–1964.

[2] A. Sari, M. Tuzen, Removal of mercury(II) from aqueous solution using moss (*Drepanocladus revolvens*) biomass: Equilibrium, thermodynamic and kinetic studies, J. Hazard. Mater. 171 (2009) 500–507.

[3] B. Ramavandi, S. Farjadfard, M. Ardjmand, Mitigation of orange II dye from simulated and actual wastewater using bimetallic chitosan particles: Continuous flow fixed-bed reactor, J. Environ. Chem. Eng. 2 (2014) 1776–1784.

[4] S. Krupa, A. Legge, Passive sampling of ambient, gaseous air pollutants: An assessment from an ecological perspective, Environ. Pollut. 107 (2000) 31–45.

[5] Q. Zhou, J. Xiao, W. Wang, G. Liu, Q. Shi, J. Wang, Determination of atrazine and simazine in environmental water samples using multiwalled carbon nanotubes as the adsorbents for preconcentration prior to high performance liquid chromatography with diode array detector, Talanta 68 (2006) 1309–1315.

[6] P.K. Malik, Use of activated carbons prepared from sawdust and rice-husk for adsorption of acid dyes: A case study of Acid Yellow 36, Dyes Pigm. 56 (2003) 239–249.

[7] G. Dotto, L. Pinto, Adsorption of food dyes acid blue 9 and food yellow 3 onto chitosan: Stirring rate effect in kinetics and mechanism, J. Hazard. Mater. 187 (2011) 164–170.

[8] P.J. Neuvonen, K.T. Olkkola, Oral activated charcoal in the treatment of intoxications, Med. Toxicol. Adverse Drug Experience 3 (1988) 33–58.

[9] B. Menale, R. Muoio, Use of medicinal plants in the South-Eastern area of the Partenio Regional Park (Campania, Southern Italy), J. Ethnopharmacol. 153 (2014) 297–307.

[10] U. Farooq, J.A. Kozinski, M.A. Khan, M. Athar, Biosorption of heavy metal ions using wheat based biosorbents—A review of the recent literature, Bioresour. Technol. 101 (2010) 5043–5053.

[11] T.A. Davis, B. Volesky, A. Mucci, A review of the biochemistry of heavy metal biosorption by brown algae, Water Res. 37 (2003) 4311–4330.

[12] Q. Feng, Q. Lin, F. Gong, S. Sugita, M. Shoya, Adsorption of lead and mercury by rice husk ash, J. Colloid Interface Sci. 278 (2004) 1–8.

[13] E. Khoramzadeh, B. Nasernejad, R. Halladj, Mercury biosorption from aqueous solutions by Sugarcane Bagasse, J. Taiwan Inst. Chem. Eng. 44 (2013) 266–269.

[14] A.S. Prudente, A.M.V. Loddi, M.R. Duarte, A.R.S. Santos, M.T. Pochapski, M.G. Pizzolatti, S.S. Hayashi, F.R. Campos, R. Pontarolo, F.A. Santos, D.A. Cabrini, M.F. Otuki, Pre-clinical anti-inflammatory aspects of a cuisine and medicinal millennial herb: *Malva sylvestris* L, Food Chem. Toxicol. 58 (2013) 324–331.

[15] J.C. Gasparetto, C.A.F. Martins, S.S. Hayashi, M.F. Otuky, R. Pontarolo, Ethnobotanical and scientific aspects of *Malva sylvestris* L.: A millennial herbal medicine, J. Pharm. Pharmacol. 64 (2012) 172–189.

[16] S. Altenor, B. Carene, E. Emmanuel, J. Lambert, J.J. Ehrhardt, S. Gaspard, Adsorption studies of methylene blue and phenol onto vetiver roots activated carbon prepared by chemical activation, J. Hazard. Mater. 165 (2009) 1029–1039.

[17] M.A. Wahab, S. Jellali, N. Jedidi, Ammonium biosorption onto sawdust: FTIR analysis, kinetics and adsorption isotherms modeling, Bioresour. Technol. 101 (2010) 5070–5075.

[18] Z. Wang, P. Yin, R. Qu, H. Chen, C. Wang and S. Ren, Adsorption kinetics, thermodynamics and isotherm of Hg(II) from aqueous solutions using buckwheat hulls from Jiaodong of China, Food Chem. 136 1508–1514.

[19] O. Hakami, Y. Zhang, C.J. Banks, Thiol-functionalised mesoporous silica-coated magnetite nanoparticles for high efficiency removal and recovery of Hg from water, Water Res. 46 (2012) 3913–3922.

[20] F. Raji, M. Pakizeh, Study of Hg(II) species removal from aqueous solution using hybrid $ZnCl_2$-MCM-41 adsorbent, Appl. Surf. Sci. 282 (2013) 415–424.

[21] T.S. Anirudhan, L. Divya, M. Ramachandran, Mercury (II) removal from aqueous solutions and wastewaters using a novel cation exchanger derived from coconut coir pith and its recovery, J. Hazard. Mater. 157 (2008) 620–627.

[22] M.B. Lohani, A. Singh, D.C. Rupainwar, D.N. Dhar, Studies on efficiency of guava (*Psidium guajava*) bark as bioadsorbent for removal of Hg (II) from aqueous solutions, J. Hazard. Mater. 159 (2008) 626–629.

[23] A. Rezaee, B. Ramavandi, F. Ganati, M. Ansari, A. Solimanian, Biosorption of mercury by biomass of filamentous algae Spirogyra species, J. Biolog. Sci. 6 (2006) 695–700.

[24] G. Asgari, B. Ramavandi, L. Rasuli, M. Ahmadi, Cr (VI) adsorption from aqueous solution using a surfactant-modified Iranian zeolite: Characterization, optimization, and kinetic approach, Desalin. Water Treat. 51 (2013) 6009–6020.

[25] G. Asgari, B. Ramavandi, S. Sahebi, Removal of a cationic dye from wastewater during purification by Phoenix dactylifera, Desalin. Water Treat. 52 (2013) 1–12.

[26] B. Ramavandi, Treatment of water turbidity and bacteria by using a coagulant extracted from *Plantago ovata*, Water Resour. Ind. 6 (2014) 36–50.

[27] G. Asgari, B. Ramavandi, S. Farjadfard, Abatement of azo dye from wastewater using bimetal-chitosan, Sci. World J. 2013 (2013) 1–10.

[28] X.S. Wang, Z.Z. Li, S.R. Tao, Removal of chromium (VI) from aqueous solution using walnut hull, J. Environ. Manage. 90 (2009) 721–729.

[29] G. Moussavi, A. Alahabadi, K. Yaghmaeian, M. Eskandari, Preparation, characterization and adsorption potential of the NH_4Cl-induced activated carbon for the removal of amoxicillin antibiotic from water, Chem. Eng. J. 217 (2013) 119–128.

[30] C. Ling, F.-Q. Liu, C. Long, T.-P. Chen, Q.-Y. Wu, A.-M. Li, Synergic removal and sequential recovery of acid black 1 and copper (II) with hyper-crosslinked resin and inside mechanisms, Chem. Eng. J. 236 (2014) 323–331.

[31] Y. Ma, Q. Zhou, S. Zhou, W. Wang, J. Jin, J. Xie, A. Li, C. Shuang, A bifunctional adsorbent with high surface area and cation exchange property for synergistic removal of tetracycline and Cu^{2+}, Chem. Eng. J. 258 (2014) 26–33.

[32] L. Carro, J.L. Barriada, R. Herrero, M.E. Sastre de Vicente, Adsorptive behaviour of mercury on algal biomass: Competition with divalent cations and organic compounds, J. Hazard. Mater. 192 (2011) 284–291.

[33] Z. Yan, H. Xue, K. Berning, Y.-W. Lam, C.-S. Lee, Identification of multifunctional graphene–gold nanocomposite for environment-friendly enriching, separating, and detecting Hg^{2+} simultaneously, ACS Appl. Mater. Interfaces 6 (2014) 22761–22768.

[34] Q. Wang, X. Chang, D. Li, Z. Hu, R. Li, Q. He, Adsorption of chromium(III), mercury(II) and lead(II) ions onto 4-aminoantipyrine immobilized bentonite, J. Hazard. Mater. 186 (2011) 1076–1081.

[35] N. Ma, Y. Yang, S. Chen, Q. Zhang, Preparation of amine group-containing chelating fiber for thorough removal of mercury ions, J. Hazard. Mater. 171 (2009) 288–293.

[36] R. Qu, C. Sun, Y. Zhang, J. Chen, C. Wang, C. Ji, X. Liu, Syntheses, characterization, and hg(II) adsorption properties of porous cross-linked polystyrene modified with 2-aminopyridine via a sulfoxide/sulfone-containing spacer arm, J. Chem. Eng. Data 55 (2010) 4343–4351.

[37] R. Li, L. Liu, F. Yang, Preparation of polyaniline/reduced graphene oxide nanocomposite and its application in adsorption of aqueous Hg(II), Chem. Eng. J. 229 (2013) 460–468.

[38] C. Green-Ruiz, Mercury(II) removal from aqueous solutions by nonviable *Bacillus* sp. from a tropical estuary, Bioresour. Technol. 97 (2006) 1907–1911.

[39] F.-N. Allouche, E. Guibal, N. Mameri, Preparation of a new chitosan-based material and its application for mercury sorption, Colloids Surf., A: Physicochem. Eng. Aspects 446 (2014) 224–232.

[40] A. Shafaei, F.Z. Ashtiani, T. Kaghazchi, Equilibrium studies of the sorption of Hg(II) ions onto chitosan, Chem. Eng. J. 133 (2007) 311–316.

[41] W. Du, L. Yin, Y. Zhuo, Q. Xu, L. Zhang, C. Chen, Performance of CuOx–neutral Al_2O_3 sorbents on mercury removal from simulated coal combustion flue gas, Fuel Process. Technol. 131 (2015) 403–408.

[42] G. Li, B. Shen, F. Lu, The mechanism of sulfur component in pyrolyzed char from waste tire on the elemental mercury removal, Chem. Eng. J. 273 (2015) 446–454.

[43] G. Li, B. Shen, Y. Wang, S. Yue, Y. Xi, M. An, K. Ren, Comparative study of element mercury removal by three bio-chars from various solid wastes, Fuel 145 (2015) 189–195.

[44] M. Arshadi, A.R. Faraji, M.J. Amiri, Modification of aluminum–silicate nanoparticles by melamine-based dendrimer l-cysteine methyl esters for adsorptive characteristic of Hg(II) ions from the synthetic and Persian Gulf water, Chem. Eng. J. 266 (2015) 345–355.